

The role of magnetic fields for planetary formation

Anders Johansen

Leiden Observatory, Leiden University, P.O. Box 9513, 2300 RA Leiden, The Netherlands
email: ajohan@strw.leidenuniv.nl

Abstract. The role of magnetic fields for the formation of planets is reviewed. Protoplanetary disc turbulence driven by the magnetorotational instability has a huge influence on the early stages of planet formation. Small dust grains are transported both vertically and radially in the disc by turbulent diffusion, counteracting sedimentation to the mid-plane and transporting crystalline material from the hot inner disc to the outer parts. The conclusion from recent efforts to measure the turbulent diffusion coefficient of magnetorotational turbulence is that turbulent diffusion of small particles is much stronger than naively thought. Larger particles – pebbles, rocks and boulders – get trapped in long-lived high pressure regions that arise spontaneously at large scales in the turbulent flow. These gas high pressures, in geostrophic balance with a sub-Keplerian/super-Keplerian zonal flow envelope, are excited by radial fluctuations in the Maxwell stress. The coherence time of the Maxwell stress is only a few orbits, where as the correlation time of the pressure bumps is comparable to the turbulent mixing time-scale, many tens or orbits on scales much greater than one scale height. The particle overdensities contract under the combined gravity of all the particles and condense into gravitationally bound clusters of rocks and boulders. These planetesimals have masses comparable to the dwarf planet Ceres. I conclude with thoughts on future priorities in the field of planet formation in turbulent discs.

Keywords. Diffusion – instabilities – MHD – planetary systems: protoplanetary disks – solar system: formation – turbulence

1. Introduction

Planets form in protoplanetary discs of gas and dust as the dust grains collide and grow to ever larger bodies (Safronov 1969). An important milestone is the formation of km-sized planetesimals. Drag force interaction between particles and gas plays a big role for the dynamics of dust particles. This way the collisional evolution of the dust grains into planetesimals is intricately connected to the physical state of the gas flow. The magnetorotational instability renders Keplerian rotation profiles linearly unstable in the presence of a magnetic field of suitable strength (Balbus & Hawley 1991). The ensuing magnetorotational turbulence is currently the best candidate for driving protoplanetary disc accretion. The relatively ease at which self-sustained magnetorotational turbulence is produced by numerical magnetohydrodynamics codes makes it an excellent test bed for analysing dust motion and formulating theories of planet formation in a turbulent environment.

An interesting constraint on the magnetic field present in the solar nebula comes from meteoritics. Most carbonaceous chondrites have a remanent magnetisation as high as a few Gauss, frozen in as the material cooled past the blocking temperature (Levy & Sonett 1978). A quote from the excellent review paper by Levy & Sonett (1978) is particularly concise on the origin of such a strong magnetic field:

“So far as we can see, there are four major candidates for the origin of the primordial magnetic field which produced the remanence in carbonaceous chondrites. They are:

1. Magnetic fields generated in very large meteorite parent bodies
2. The interstellar magnetic field compressed to high intensity by the inflowing gas
3. A strong solar magnetic field permeating the early solar system
4. A hydromagnetic dynamo field produced in the gaseous nebula itself”

Levy & Sonett (1978) continue to put forward various physical arguments to rule out possibility 1 and 2 [the undifferentiated parent bodies of carbonaceous chondrites were unlikely to harbour a magnetic field, and turbulent diffusion strongly limits the amount of field that can be dragged into the solar nebula (Lubow *et al.* 1994)]. The magnetic field of the wind emanating from the young sun can potentially be strong enough to imprint fields of several G at a few AU from the sun. But the most likely scenario remains that the magnetic field was created by the differential rotation and dynamo process in the solar nebula itself. Simulations of magnetised shear flows indeed show that a weak seed field can be amplified by the magnetorotational instability to a few percent of the thermal pressure (Brandenburg *et al.* 1995, Hawley *et al.* 1996, Sano *et al.* 2004).

In the following sections I briefly review the role of such magnetised turbulence on the motion of dust particles and on the cosmogony of planetesimal formation.

2. Diffusion of small dust grains

The magnetised turbulence in protoplanetary discs moves small dust grains around, preventing them from sedimenting to the mid-plane and transporting dusty material radially in the disc (Gail 2002, van Boekel *et al.* 2004). This section describes recent efforts to determine the turbulent diffusion coefficient D_t of magnetorotational turbulence.

If turbulent transport can be described as a diffusion process, then the evolution of the dust particle density ρ_d follows the partial differential equation

$$\frac{\partial \rho_d}{\partial t} = \nabla \cdot \left[D_t \rho_g \nabla \left(\frac{\rho_d}{\rho_g} \right) \right]. \quad (2.1)$$

Here ρ_g is the gas density, its presence signifying that diffusion acts to even out differences in the solids-to-gas ratio $\epsilon_d = \rho_d / \rho_g$. The vertical flux of dust particles contains contributions from the advection (sedimentation at velocity w_z) and the diffusion,

$$\mathcal{F}_z = w_z \rho_d - D_t \rho_g \frac{\partial (\rho_d / \rho_g)}{\partial z}. \quad (2.2)$$

In sedimentation-diffusion equilibrium we have $\mathcal{F}_z = 0$. Setting the velocity of the dust particles its terminal value, $w_z = -\tau_f \Omega^2 z$ (where Ω is the Keplerian frequency and τ_f is the friction time of the particles), gives the solution (e.g. Dubrulle *et al.* 1995)

$$\epsilon_d(z) = \epsilon_1 \exp[-z^2 / (2H_\epsilon^2)] \quad (2.3)$$

for the solids-to-gas ratio $\epsilon_d = \rho_d / \rho_g$. The scale height H_ϵ follows the expression

$$H_\epsilon^2 = \frac{D_t}{\tau_f \Omega^2}, \quad (2.4)$$

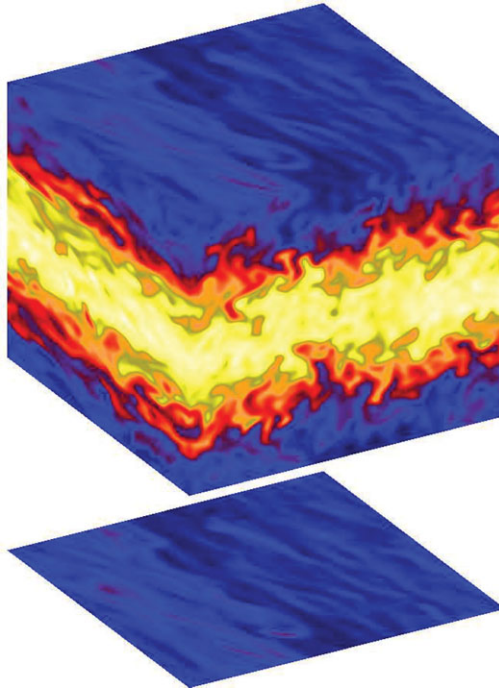


Figure 1. The dust density at the sides of a simulation box corotating with the disc at an arbitrary distance from the central star. The radial direction points right, the azimuthal direction left and up, while the vertical direction points directly up. The dust density distribution arises from an equilibrium between sedimentation and turbulent diffusion by the magnetorotational turbulence.

while the solids-to-gas ratio in the mid-plane is given by

$$\epsilon_1 = \epsilon_0 \sqrt{\left(\frac{H}{H_\epsilon}\right)^2 + 1}. \quad (2.5)$$

Here H is the pressure scale height of the gas. In the above derivations we have assumed (a) that the friction time is independent of height over the mid-plane and (b) that the diffusion coefficient is independent of height over the mid-plane. None of these assumptions are true in general, but if we stay within a few scale heights of the mid-plane and treat the diffusion coefficient as a suitably averaged diffusion coefficient, then the expressions are relatively good approximations.

In a real turbulent flow the observed diffusion-sedimentation equilibrium can be used to measure the turbulent diffusion coefficient of the flow. In Figure 1 we show an example of such a diffusion-sedimentation equilibrium (from Johansen & Klahr 2005) for a shearing box simulation of magnetorotational turbulence. The problem of determining the diffusion coefficient is thus reduced to measuring the scale height H_ϵ of the dust in Figure 1. Using equation 2.4 then directly yields a value of D_t . Obviously the diffusion coefficient must scale with the overall strength of the turbulence. The interesting quantity to determine is thus the Schmidt number Sc , defined as the turbulent viscosity coefficient relative to the turbulent diffusion coefficient, $Sc = \nu_t/D_t$. In a Keplerian disc the turbulent viscosity is in turn defined from the Reynolds and Maxwell stresses,

$$\nu_t = \frac{2}{3} \frac{\langle \rho u_x u_y - \mu_0^{-1} B_x B_y \rangle}{\langle \rho \rangle} \quad (2.6)$$

The Schmidt number was found by Johansen & Klahr (2005) to be around 1.5 for vertical diffusion and 0.85 for radial diffusion. This is surprisingly close to unity and a bit mysterious given that the turbulent viscosity is dominated by the magnetic Maxwell stress $\langle -\mu_0^{-1} B_x B_y \rangle$. This stress does not directly affect the dust particles. A possible explanation is that diffusion is determined by the diagonal entries in the $u_i u_j$ correlation tensor. These are much higher than the off diagonal Reynolds stress $u_x u_y$. Thus the MRI inherently transports a passive scalar (by fluid motion) and the angular momentum (by magnetic tension) equally well.

Different groups have used various independent methods to measure the turbulent diffusion coefficient of magnetorotational turbulence. A vertical Schmidt number of around unity was measured by Turner *et al.* (2006), while Fromang & Papaloizou (2006) reported a value of approximately three. This gives some confidence that the Schmidt number is well constrained. However, Carballido *et al.* (2005) found a radial Schmidt number as high as ten in relatively strong turbulence. To address the discrepancy between this value and the much lower value found by Johansen & Klahr (2005), Johansen *et al.* (2006b) performed simulations of the MRI with various strengths of an imposed, external field, yielding a higher turbulent viscosity than in zero net flux simulations. The Schmidt number was indeed found to decrease with increasing strength of the turbulence. Stronger turbulence (such as in Carballido *et al.* 2005) is less good at diffusing dust particles relative to its stresses. The explanation is that the correlation time of the turbulence decreases with increasing turbulent energy, and that turbulent structures do not stay coherent long enough to effectively diffuse particles.

Large particles partially decouple from the turbulence and are primarily diffused by large scale eddies with relatively long correlation times. The experiments by Carballido *et al.* (2006) indeed showed that the diffusion coefficient falls rapidly for particles above a few metres in size, in good agreement with the analytical derivations of Youdin & Lithwick (2007).

3. Zonal flows

While smaller dust particles are clearly prevented from forming a very thin mid-plane layer by the magnetorotational turbulence, pebbles, rocks and boulders begin to gradually decouple from the gas. Accretion discs are radially stratified with a pressure that decreases with distance from the star. The pressure gradient acts to reduce the effect of gravity felt by the gas, and as a result the gas rotates slightly slower than Keplerian. The particles, however, do not react to gas pressure gradients and aim to orbit with the Keplerian speed. The head wind of the slower rotating gas drains the particles of angular momentum and they spiral towards the star in a few hundred orbital periods (Weidenschilling 1977).

The radial pressure profile of gas in turbulent discs need not be monotonously falling. The presence of large scale, long-lived pressure bumps leads to concentrations of migrating dust particles into radial bands. Simulations of magnetorotational turbulence in a box gives evidence that such pressure bumps form spontaneously in the turbulent flow (Johansen *et al.* 2006, Johansen *et al.* 2009). In Figure 2 we plot the gas density and the azimuthal velocity, averaged over the azimuthal and vertical directions, as a function of radial distance from the centre of the box x and the time t . The gas density exhibits axisymmetric column density bumps with amplitude around 5% of the average density. These bumps are surrounded by a sub-Keplerian/super-Keplerian zonal flow, maintaining perfect geostrophic balance with $2\rho_0\Omega u_y \approx \partial P/\partial r$.

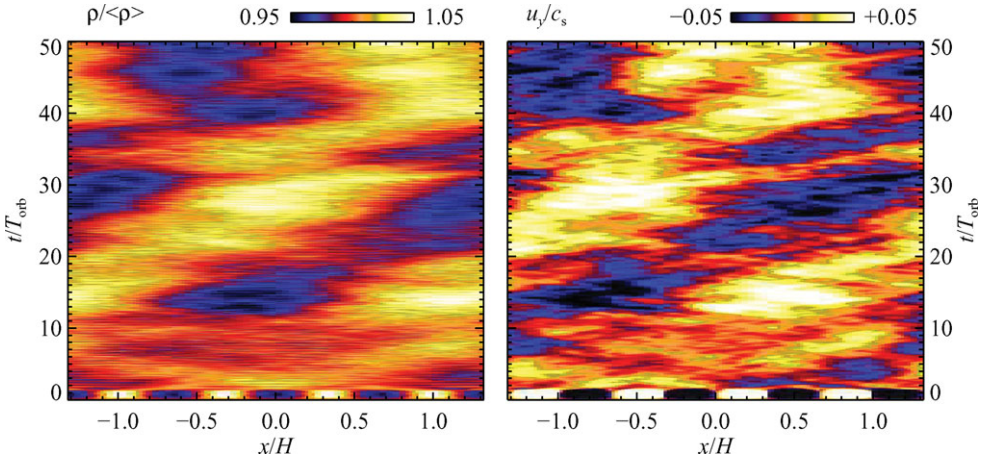


Figure 2. The gas density (left plot) and the azimuthal velocity (right plot) as a function of the radial distance from the centre of the box, H , and the time, t , measured in orbits. There is a perfect $-\pi/2$ phase difference between the pressure bump and the zonal flow, in agreement with a geostrophic balance. The zonal flow has in turned been excited by a large scale variation in the Maxwell stress.

Varying resolution, presence or non-presence of stratification, dissipation parameters and dissipation types, Johansen *et al.* (2009) find that pressure bumps and zonal flows are ubiquitous in shearing box simulations of magnetorotational turbulence, provided that the simulation box is large enough (more than one scale height in radial extent) and possibly also that the physical dissipation is high enough. What is then the launching mechanism for these zonal flows? Large scale fluctuations in the Maxwell stress lead to a differential transport of momentum. Thus the magnetic field is responsible for separating the orbital flow into regions of slightly faster and slightly slower rotation.

A model of the excitation of zonal flows and pressure bumps can be obtained from a simplified version of the dynamical equations,

$$0 = 2\Omega\hat{u}_y - \frac{c_s^2}{\rho_0}ik_0\hat{\rho}, \tag{3.1}$$

$$\frac{d\hat{u}_y}{dt} = -\frac{1}{2}\Omega\hat{u}_0 + \hat{T}, \tag{3.2}$$

$$\frac{d\hat{\rho}}{dt} = -ik_0\hat{u}_x - \frac{\hat{\rho}}{\tau_{\text{mix}}}. \tag{3.3}$$

Here \hat{u}_x , \hat{u}_y and $\hat{\rho}$ are the amplitudes of the radial and azimuthal velocity and gas density at the largest radial scale of the simulation, with wavenumber k_0 . The first equation denotes geostrophic balance, while we have kept the time evolution terms in the two other equations. Non-linear terms enter through \hat{T} , the large scale magnetic tension, and $\hat{\rho}/\tau_{\text{mix}}$, turbulent diffusion of the mass density.

We can combine the above equations into a single evolution equation for the density,

$$\frac{d\hat{\rho}}{dt} = \frac{1}{1+k_0^2H^2} \left(\hat{F} - \frac{\hat{\rho}(t)}{\tau_{\text{mix}}} \right), \tag{3.4}$$

where $\hat{F} \equiv -2ik_0\rho_0\hat{T}/\Omega$ is the forcing term. The prefactor $c_k \equiv (1+k_0^2H^2)^{-1}$ is a pressure correction for small-scale modes that both decreases the amplitude of the forcing and increases the effective damping time. The coherence time-scale of the Maxwell stress (and thus of \hat{F}), τ_{for} , is generally much shorter than the mixing time-scale, τ_{mix} . Thus we need

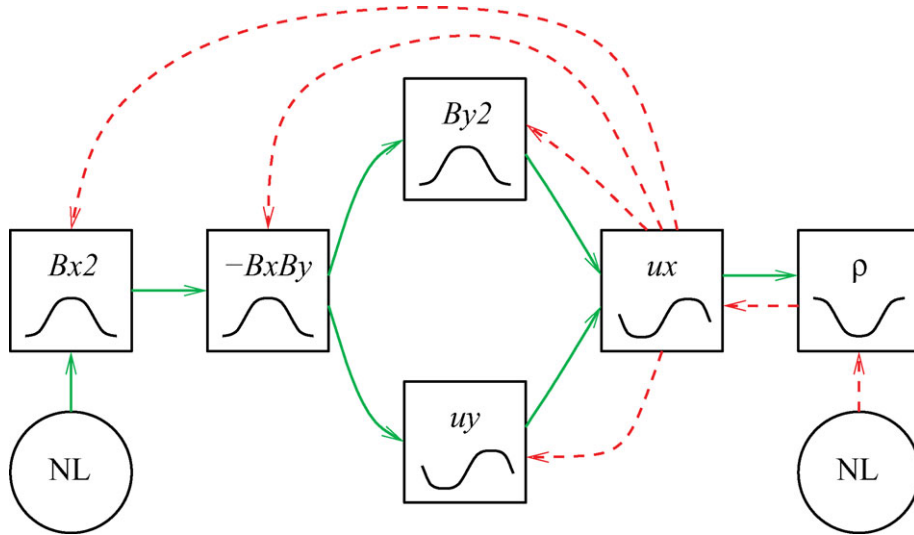


Figure 3. Diagram of how non-linear excitation of the large scale radial magnetic energy leads to the excitation of zonal flow. Green arrows label positive energy transfer, while red arrows (dashed) denote energy sinks. Non-linear interactions are responsible both for the excitation and for the balance, the latter through diffusive mixing of the gas density.

to model equation 3.4 as a stochastic differential equation (see e.g. Youdin & Lithwick 2008). The Maxwell stress gives short, uncorrelated kicks to the zonal flow. This would lead to an amplitude that grows as the square root of time. However, in presence of turbulent diffusion, the solution tends to

$$\frac{\hat{\rho}_{\text{eq}}}{\rho_0} = 2\sqrt{c_k \tau_{\text{tor}} \tau_{\text{mix}}} H k_0 \frac{\hat{T}}{c_s}. \quad (3.5)$$

The correlation time of the zonal flows is predicted to be equal to the mixing time-scale, in good agreement with the results. The model also predicts that $\hat{\rho}_{\text{eq}} \propto k^{-2}$ for $k_0 H \gg 1$. This is in very good agreement with the very clearly sinusoidal density fluctuations seen in Figure 2.

The cause of the large scale variation in the Maxwell stress remains unknown. Johansen *et al.* (2009) argue that magnetic energy takes part in an inverse cascade from the moderate scales, excited directly by the MRI, to large scales. A diagram of the zonal flow excitation appears in Figure 3. Note that the above zonal flow excitation model assumes that the magnetic tension (i.e. $-B_x B_y$ in Figure 3) is given, whereas in fact one may go on step further back to B_x^2 , which is excited directly by a non-linear term. The Maxwell stress then increases from the Keplerian stretching of the radial field. The model also predicts that the magnetic pressure should grow in anti-phase with the thermal pressure. This is indeed also observed.

4. Planetesimal formation

The zonal flows presented in the last section are very efficient at trapping particles. At the outer sub-Keplerian side the particles face a slightly stronger headwind and drift faster inwards. At the inner super-Keplerian side the particles experience a slight backwind and move out. The effect of pressure bumps on the migration of rocks and boulders goes at least back to Whipple (1972). It has later received extensive analytical treatment

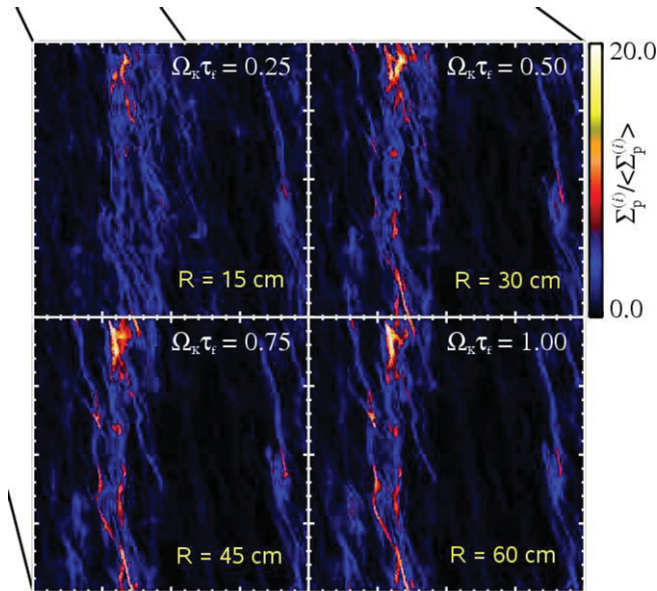


Figure 4. The column density of four different particle sizes, before self-gravity has been switched on. The particles concentrate at the same locations, but larger particles experience a higher local column density.

by Klahr & Lin (2001) and by Haghighipour & Boss (2003). The narrow box simulations of Hodgson & Brandenburg (1998) found no evidence for long-lived concentrations of relatively tightly coupled particles in magnetorotational turbulence. However, Johansen *et al.* (2006a) observed concentrations of marginally coupled dust particles (cm-m sizes), by up to two orders of magnitude higher than the average particle density, in high pressure regions occurring in magnetorotational turbulence. In a simulation of a (part of a) global disc Fromang & Nelson (2005) reported similar concentrations in a long-lived vortex structure.

The question of how long-lived high pressure structures form and survive in magnetised turbulence is of general interest. However, their effect on planetesimal formation is no less intriguing. Johansen *et al.* (2007) expanded earlier models of boulders in turbulence by considering several particle sizes simultaneously and solving for the self-gravity of the boulders. First the turbulence is allowed to develop for 20 local rotation periods without the gravity of the particles (which is weak anyway). This way a sedimentary mid-plane layer, with a width of a few percent of the gas scale height, forms in equilibrium between sedimentation and turbulent diffusion. In Figure 4 we show the column density of the four different particle sizes – rocks and boulders with sizes 15 cm, 30 cm, 45 cm, and 60 cm. A weak zonal flow has been sufficient to create bands of very high particle overdensity. An additional instability in the coupled motion of gas and dust has further augmented the local overdensities (Goodman & Pindor 2000, Youdin & Goodman 2005, Youdin & Johansen 2007, Johansen & Youdin 2007).

As the self-gravity of the disc is activated, the overdense bands contract radially. Upon reaching the local Roche density, a full non-axisymmetric collapse occurs and a few gravitationally bound clusters of rocks and boulders condense out of the particle layer. The column density of the particles is shown in Figure 5.

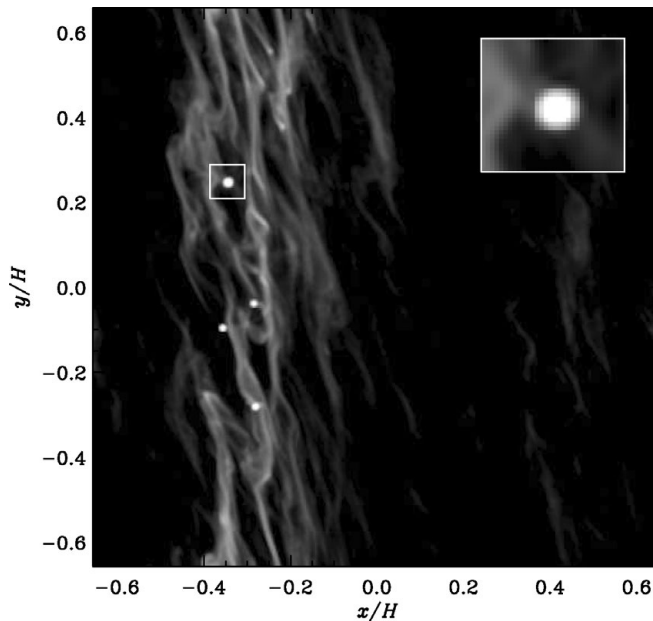


Figure 5. The column density at $\Delta t = 7T_{\text{orb}}$ after self-gravity is turned on. Four gravitationally bound clusters of rocks and boulders have condensed out of the flow. The most massive cluster (see enlargement) has a mass comparable to the dwarf planet Ceres by the end of the simulation.

5. Conclusions

The presence of magnetic fields in protoplanetary discs is of vital importance for planet formation and for observational properties of protoplanetary discs. Small dust grains are transported very efficiently by the turbulence. While this counteracts sedimentation to the mid-plane, and thus prevents the razor thin mid-plane layer of Goldreich & Ward (1973) from forming, the turbulent transport underlies the presence of small dust grains many scale heights above the disc mid-plane. The presence of crystalline silicates in the cold outer regions of discs (Gail 2002, van Boekel *et al.* 2004) can likely also be attributed to turbulent diffusion (but see Dullemond *et al.* 2006 for an alternative view taking into account disc formation history).

Larger dust particles – pebbles, rocks, and boulders – slow down or reverse the radial migration as they encounter variations in the radial pressure gradient. Fluctuations in the Maxwell stress, with a coherence time of a few orbits, launch axisymmetric zonal flows. These flows in turn go into geostrophic balance with a radial pressure bump. The concentrations of solid particles in such pressure ridges can get high enough for a gravitational collapse into planetesimals to occur. However, a satisfactory mechanism for setting the scale of the pressure bumps is lacking, as the bumps grow to fill the box for all considered box sizes in Johansen *et al.* (2009). The final size may ultimately be set by global curvature effects (Lyra *et al.* 2008a).

An important problem related to the motion of dust particles in turbulence is their collision speeds. The relative speed of small particles approaches zero as the particle separation is decreased. But particles that are only marginally coupled to the turbulent eddies have a significant memory of their trajectories and can collide at non-zero speeds. Carballido *et al.* (2008) indeed found that the relative speeds of large particles is unchanged below a certain separation, giving confidence that the proper collision speed has been found. Turbulent eddies with sizes around the stopping length of the particle are

most efficient at inducing relative motion. However, even for marginally coupled particles these eddies may be on the edge of the dissipative subranges of the turbulence, due to the limited resolution of numerical simulations. Johansen *et al.* (2007) found that the collision speed, measured as the velocity difference over a single grid cell, increases by 10–20% each time the resolution is doubled. Ultrahigh resolution measurements of large scale and short scale relative speeds, and comparison to analytical models (Völk *et al.* 1980, Cuzzi *et al.* 1993, Schräpler & Henning 2004, Youdin & Lithwick 2008) and to sticking experiments (Wurm *et al.* 2006, Blum & Wurm 2008), is an important future priority for our picture of how planets form in turbulent gas discs.

To our best knowledge parts of the solar nebula had so low ionisation fraction that the collisional resistivity was too high for the magnetorotational instability to develop (e.g. Gammie 1996, Sano *et al.* 2000). Kretke & Lin (2007) and Brauer *et al.* (2008) modelled the sharp increase in resistivity as the gas temperature drops below the freezing point of ice (the so-called snow line) at a few AU from the sun. The corresponding drop in turbulence activity leads to a pile up of gas and a run away growth in particle density from the influx of migrating solid particles. The lack of radial drift in such a location allows for planetesimal formation by coagulation to occur without having to compete with the radial drift time-scale. The edges of “dead zones” can be unstable to a Rossby wave instability (Inaba & Barge 2006, Varnière & Tagger 2006). The Rossby vortices efficiently trap particles, which leads to a burst of planet formation at the edge of dead zones (Lyra *et al.* 2008b). This way magnetic fields helps the planet formation process both in their presence and in their absence.

Acknowledgements

I would like to thank my collaborators Andrej Bicanski, Andrew Youdin, Axel Brandenburg, Frithjof Brauer, Hubert Klahr, Jeff Oishi, Kees Dullemond, Mordecai-Mark Mac Low, Thomas Henning, and Wladimir Lyra.

References

- Balbus, S. A. & Hawley, J. F. 1991, *ApJ* 376, 21
Blum, J. & Wurm, G. 2008, *ARA&A* 46, 21
Brauer, F., Henning, T., & Dullemond, C. P. 2008, *A&A* 487, L1
Brandenburg, A., Nordlund, Å., Stein, R.F., & Torkelsson, U. 1995, *ApJ* 446, 741
Carballido, A., Stone, J. M., & Pringle, J. E. 2005, *MNRAS* 358, 1055
Carballido, A., Fromang, S., & Papaloizou, J. 2006, *MNRAS* 373, 1633
Carballido, A., Stone, J. M., & Turner, N. J. 2008, *MNRAS* 386, 145
Cuzzi, J. N., Dobrovolskis, A. R., & Champney, J. M. 1993, *Icarus* 106, 102
Dubrulle, B., Morfill, G., & Sterzik, M. 1995, *Icarus* 114, 237
Dullemond, C. P., Apai, D., & Walch, S. 2006, *ApJ* 640, L67
Fromang, S. & Nelson, R. P., 2005, *MNRAS* 364, L81
Fromang, S. & Nelson, R. P. 2006, *A&A* 457, 343
Fromang, S. & Papaloizou, J. 2006, *A&A* 452, 751
Gail, H.-P. 2002, *A&A* 390, 253
Gammie, C. F. 1996, *ApJ* 457, 355
Goldreich, P. & Ward, W. R., 1973, *ApJ* 183, 1051
Goodman, J. & Pindor, B. 2000, *Icarus* 148, 537
Haghighipour, N., & Boss, A. P., 2003, *ApJ* 598, 1301
Hawley, J. F., Gammie, C. F., & Balbus, S. A. 1996, *ApJ* 464, 690
Hodgson, L. S. & Brandenburg, A. 1998, *A&A* 330, 1169
Inaba, S. & Barge, P. 2006, *ApJ* 649, 415

- Johansen, A. & Klahr, H. 2005, *ApJ* 634, 1353
- Johansen, A., Klahr, H., Henning, Th. 2006, *ApJ* 636, 1121
- Johansen, A., Klahr, H., & Mee, A. J. 2006c, *MNRAS* 370, L71
- Johansen, A., Oishi, J. S., Low, M.-M. M., Klahr, H., Henning, T., & Youdin, A. 2007, *Nature* 448, 1022
- Johansen, A. & Youdin, A. 2007, *ApJ* 662, 627
- Johansen, A., Youdin, A., & Klahr, H. 2009, *ApJ*, submitted
- Klahr, H. H. & Lin, D. N. C., 2001, *ApJ* 554, 1095
- Kretke, K. A. & Lin, D. N. C. 2007, *ApJ* 664, L55
- Levy, E. H. & Sonett, C. P. 1978, in: T. Gehrels (ed.), *IAU Colloquium 52: Protostars and Planets* (The University of Arizona Press), p. 516
- Lubow, S. H., Papaloizou, J. C. B., & Pringle, J. E. 1994, *MNRAS* 267, 235
- Lyra, W., Johansen, A., Klahr, H., & Piskunov, N. 2008, *A&A* 479, 883
- Lyra, W., Johansen, A., Klahr, H., & Piskunov, N. 2008, *A&A* 491, L41
- Safronov, V. S. 1969, *Evoliutsiia doplanetnogo oblaka* (Nakua)
- Sano, T., Miyama, S. M., Umebayashi, T., & Nakano, T. 2000, *ApJ* 543, 486
- Sano, T., Inutsuka, S.-i., Turner, N. J., & Stone, J. M. 2004, *ApJ* 605, 321
- Turner, N. J., Willacy, K., Bryden, G., & Yorke, H. W. 2006, *ApJ* 639, 1218
- van Boekel, R., *et al.* 2004, *Nature* 432, 479
- Varnière, P. & Tagger, M. 2006, *A&A* 446, 13
- Völk, H. J., Morfill, G. E., Roeser, S., & Jones, F. C. 1980, *A&A* 85, 316
- Weidenschilling, S. J. 1977, *MNRAS* 180, 57
- Whipple, F. L. 1972, in: A. Elvius (ed.), *From Plasma to Planet* (Wiley Interscience Division), p. 211
- Wurm, G., Paraskov, G., & Krauss, O. 2005, *Icarus* 178, 253
- Youdin, A. N. & Goodman, J. 2005, *ApJ* 620, 459
- Youdin, A. N. & Johansen, A. 2007, *ApJ* 662, 613
- Youdin, A. N. & Lithwick, Y. 2007, *Icarus* 192, 588

Discussion

BLACKMAN: There has been recent evidence that the Maxwell stress resulting from the MRI scales with box size for small boxes. Have you been able to see a saturation of the Maxwell stress in combining your large radial scale and multi-scale height (in vertical direction) boxes? One would expect that boxes that allow field structures with $H \approx R$ are required.

JOHANSEN: Yes, we have seen such a saturation in the Maxwell stress. When changing the radial and azimuthal extent of the box from $L_x = L_y = 1.32H$ to $L_x = L_y = 2.64H$ the Maxwell stress increases from ≈ 0.005 to ≈ 0.01 . However, another doubling at the box size yields no further change to the Maxwell stress.